Bistable buckled beam and force actuation: Experimental validations

CrossMark

B. Camescasse, A. Fernandes *, J. Pouget [1]

UPMC Univ Paris 06, UMR 7190, Institut Jean Le Rond d'Alembert, F-75005 Paris, France
CNRS, UMR 7190, Institut Jean Le Rond d'Alembert, F-75005 Paris, France

ARTICLE INFO

ABSTRACT

This paper presents recent experimental results on the switching of a simply supported buckled beam. Moreover, the present work is focussed on the experimental validation of a switching mechanism of a bistable beam presented in details in Camescasse et al. (2013). An actuating force is applied perpendicularly to the beam axis. Particular attention is paid to the influence of the force position on the beam on the switching scenario. The experimental set-up is described and special care is devoted to the procedure of experimental tests highlighting the main difficulties and how these difficulties have been overcome. Two situations are examined: (i) a beam subject to mid-span actuation and (ii) off-center actuation. The bistable beam responses to the loading are experimentally determined for the buckling force and actuating force as a function of the vertical position of the applied force (displacement control). A series of photos demonstrates the scenarios for both situations and the bifurcation between buckling modes are clearly shown, as well. The influence of the application point of the force on the bifurcation force is experimentally studied which leads to a minimum for the bifurcation actuating force. All the results extracted from experimental tests are compared to those coming from the modeling investigation presented in a previous work (Camescasse et al., 2013) which ascertains the proposed model for a bistable beam.

© 2014 Elsevier Ltd. All rights reserved.

1. Introduction

A slender elastic beam subject to buckling load is a very simple candidate to design a bistable mechanism. In spite of its apparent basic deformation, such a system possesses relative complexity due to mainly its nonlinearity and instability phenomenon. In a previous work, the authors (Camescasse et al., 2013) reported an analytical study of a bistable system made of a simply supported elastic beam and loaded by a compressive force in its axis direction. The model is based on the elastica theory of beams. The model accounts for large transformations (in particular, a cross-section rotation of large amplitudes) as well as the extensibility property of the beam. In the present work we propose experimental validations of the switching process of the bistable beam under the actuation of localized force.

There has been considerable effort devoted to the design and manufacturing of bistable micro-mechanisms for micro-valves (Goll et al., 1996; Schomburg and Goll, 1998), micro-switches or relays (Matoba et al., 1994; Vangbo and Bäklund, 1998; Jensen et al., 1999; Saif, 2000; Baker and Howell, 2002), fiber-optic switches, digital micro-mirrors (Maekoba et al., 2001) and mechanical memories. More research relies on a bistable buckled beam. This particular class of bistable mechanisms uses deflection to amplify deformation of the elastic beam. The essential advantage of this class of mechanisms remains in stable equilibrium in two distinct positions. This interesting behavior is valuable for micro-mechanical application because power is applied only to have the bistable switched from one stable position to the other one and the state of the system is not lost upon interruption of the power to the system. Magnetically actuated devices are well adapted for actuating bistable mechanisms and used to design MEMS with low energy supply (Gray and Kohl, 2005; Gray et al., 2005). The design of micro- and nano-mechanical devices using bistable beams subject to different kinds of actuation becomes very attractive for systems requiring low level of power consumption and their ability to be miniaturized. Charlot et al. present a micro-mechanical pre-stressed bistable beam of few micro-meters of length to be used as a non-volatile mechanical memory (Charlot et al., 2008). In their work, the actuation of the micro-beam is based on an electrostatic force by applying a voltage to two separate electrodes on each side of the beam. Models for electrically actuated MEMS have been examined by Das and Batra (Das and Batra, 2009). They analyze a perfect electrically conducting

* Corresponding author at: UPMC Univ Paris 06, UMR 7190, Institut Jean Le Rond d'Alembert, F-75005 Paris, France.

E-mail addresses: amancio.fernandes@upmc.fr (A. Fernandes), pouget@lmm.jussieu (J. Pouget).

[1] Principal corresponding author.

clamped–clamped arch subject to electrostatic force due to a difference of electric potential between a semi-infinite rigid electrode and a deformed beam. Finite element simulations are compared to experimental tests. Park and Hah (Park and Hah, 2008) study analytically and experimentally the actuation of a pre-shaped buckled beam controlled by electromagnetic forces.

Among bistable mechanisms, the pseudo-rigid-body model provides an interesting approach useful for the analysis of compliant systems. This kind of model consists of compliant segments using two or more rigid segments joined by rigid-body joints with springs at the joints to model segment's stiffness (Howell et al., 1996; Edwards et al., 2001; Jensen and Howell, 2004). In the present work, the bistable system is merely a buckled elastic beam which is initially straight. However, it is interesting to report that structures such as shallow elastic arches can be considered in the design of bistable systems. A pioneering experimental study of mode instabilities of elastic arches was conducted by Pippard (Pippard, 1990). Further experimental evidence of instability phenomena of buckled beam or elastic arches were performed by Chen and Su (Chen and Su, 2011). Qiu and co-authors (Qiu et al., 2001) consider a micro-system made of a centrally-clamped parallel bistable beam to showcase the theoretical prediction of the snap-through for central actuation. A study close to the present work has been proposed by Chen and Hung (Chen and Hung, 2011). In their work the authors examine the mid-span actuation and snapping effect of an elastic arch by a localized force. The study focuses on the way of applying the force with respect to the mid-span of the beam. In addition, experimental observations are compared to the theoretical predictions.

In the present study there has been an effort to bridge the modeling phase of a bistable buckled beam (Camescasse et al., 2013) and experimental observations. The emphasis is especially placed on the bifurcation phenomena and the beam response under a localized force. In the next section, we recall the essential ingredients of the theoretical model, the beam geometrical, material parameters, and the loading conditions. In addition, the presentation of the numerical algorithm which has been used to obtain the numerical results of the model is briefly reported. Section 3 is devoted to experimental study. The section first presents, in detail, the experimental set-up. The experimental observations and results are reported for the bifurcation diagram and the bistable response in force–displacement for mid-span and off-center actuations. The experimental results are accompanied by photographs helping us to demonstrate the role played by the buckling modes in the switching process. The final section underlines the most pertinent results and proposes further studies.

2. Description of the system and modeling

We consider a simply supported initially straight elastic beam $[AB]$ of length L_0, width b and thickness h. The fixed Cartesian reference frame $\mathcal{R}_0(A; \vec{e}_1, \vec{e}_2, \vec{e}_3)$ is set such that the x-axis coincides with the neutral axis of the beam, and takes place in the (x, y) plane. The z-axis is then perpendicular to the plane deformation, see Fig. 1.

Under an axial compression P the right end moves towards the left end and the elastic beam buckles. The small-deflection hypothesis is still valid and the distance between the pin-joints becomes $L = L_0 - \Delta L$.

The elastic behavior of the beam is supposed to be linear. The homogeneous beam with Young modulus E, A and I respectively, the cross-sectional area, and the moment of inertia of the cross-section along the z-axis is then actuated to switch from one stable state to the other one by an actuating force $\vec{F} = -F\vec{e}_2$ applied at the point C $(x(s_C) = x_C)$.
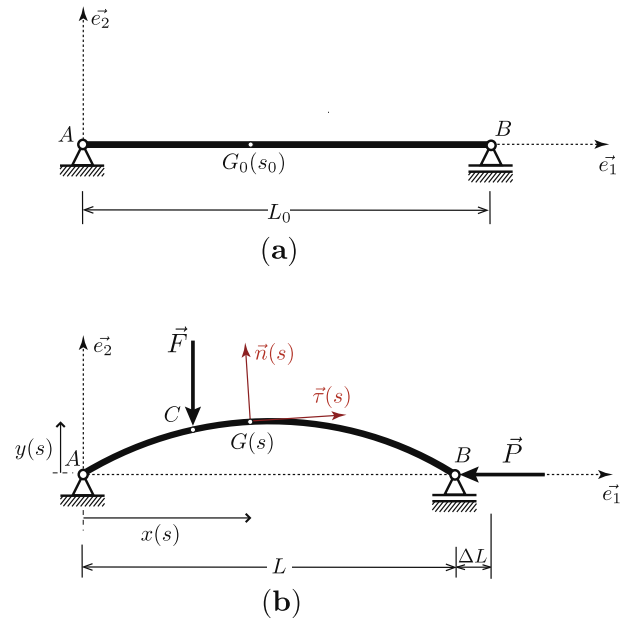

Fig. 1. Simply supported elastic beam: (a) the non loaded beam, (b) the beam in its buckled configuration with the actuating force.

We note by s the curvilinear abscissa along the beam axis in the reference configuration. The unit vector tangential to the current axis of the deformed beam at the point $G(s)$ $\vec{\tau}$ is defined by

$$\vec{\tau}(s) = \frac{d\overrightarrow{AG}}{ds} = x'(s)\,\vec{e}_1 + y'(s)\,\vec{e}_2 = \cos\theta(s)\,\vec{e}_1 + \sin\theta(s)\,\vec{e}_2 \qquad (1)$$

where $\theta(s) = (\vec{e}_1, \vec{\tau}(s))$ is the angle of rotation.

On using Eq. (1), the constitutive equations and the beam equations, the static equation for the present buckling beam (valid for both segments $[0, s_C[$ and $]s_C, L_0]$) takes on the form (Camescasse et al., 2013)

$$EI\,\theta''(s) + \delta^{\pm}\,F\cos\theta(s) + P\sin\theta(s)$$
$$- \frac{1}{EA}\left[\delta^{\pm}PF\cos(2\theta(s)) - \frac{1}{2}\left(P^2 - (\delta^{\pm})^2 F^2\right)\sin(2\theta(s))\right] = 0. \qquad (2)$$

with
$$\begin{cases} \delta^- = \delta - 1, & \forall s \in [0, s_C[\\ \delta^+ = \delta, & \forall s \in]s_C, L_0] \end{cases}$$

where the parameter δ denotes the ratio $\delta = \frac{x_C - x_A}{x_B - x_A}$, the relative position of the point C with respect to the support distance.

The nonlinear boundary value problem given by Eq. (2) along with boundary conditions at each end of the beam is solved by using a continuation algorithm based on shooting method combined with a predictor–corrector algorithm to find the shooting parameters (Camescasse et al., 2013).

3. Experimental results and validations

This Section reports a set of results extracted from the experimental tests concerning the bistable beam modeling and the switching process using localized force. The first experimental study deals with the bifurcation diagram which is the basic result for the beam buckling. The following experimental study concerns the force–displacement response of the bistable beam subject to localized force applied perpendicularly to the beam axis. Two situations are examined: (i) an actuating force localized at the mid-span beam and (ii) an off-center actuation. The influence of

the actuating position on the force–displacement curves is examined in order to find the existence of optimal position in terms of force at the bifurcation point of the force–displacement diagram. According to the modeling part of the work (Camescasse et al., 2013), the bifurcation force can be defined as the force for which the path of the bistable response changes from the stable branch to the unstable one and *vice versa*. Comparisons to the results coming from the modeling study are discussed for each situation.

3.1. Technical details about the experimental set-up

3.1.1. Material

The thin elastic beam is made of stainless steel $A301$ with a Young modulus of $E = 207$ GPa, length of 200 mm, width of 13 mm and thickness of 0.4 mm. The thin elastic beams are manufactured from a sheet of stainless steel using an electro-eroding process. Several test beams have been cut with an accuracy of 5/100 mm. Particular attention is paid to obtaining a high quality of planar beams with a minimum of residual stress. The beam is heated at 500 °C in an oven for a few hours and maintained absolutely planar and then cooled gradually to the ambient temperature.

3.1.2. Experimental set-up

The thin beam is placed between two axes made of small tubes with slots corresponding to the beam thickness. The beam is maintained fixed at each end, however the ends of the beam can freely rotate around the tube axis. The tubes are placed between two high-precision screws equipped with a small ball inserted at one of the extremities in order to adjust the tubes to be perfectly parallel and to form a spherical joint. The test set-up is equipped with a micrometric translator at the one end. The translators allow us to control the displacement of one end of the beam while the other is maintained fixed. Using a ThorLabs® PT-1 travel translator stage we are able to control the end-shortening of the beam with a 10 μm adjustment. Fig. 2 shows the photo of the complete experimental set-up equipped with the force measurement apparatus.

For the measurement of the axial compressive force which maintains the beam end-shortening fixed we use force sensor of Sensel Measurement® of the SM2 model (an S-shaped force sensor with four strain gauges). The force sensor is connected to amplifier to convert the force sensor output voltage to a signal to be analyzed with a multimeter. The sensitivity tolerance of the sensor is less than ±0.1 % with a good linearity and low hysteresis. The force sensor was calibrated before the tests which ensures an excellent degree of accuracy. The main drawback of the procedure is the force sensor deformation imposed by the travel translator as the buckling loading of the beam is increased. Accordingly, the end-shortening of the beam does not exactly correspond to the one displayed by the micrometer of the translator. We must account for the deformation of the force sensor. Fig. 3 shows the force applied to the sensor as a function of its shortening. We note, in Fig. 3, that the force sensor has an excellent linearity and that there is no hysteresis. It is worthwhile noting that the maximum of compressive deformation of the force sensor is approximately 0.25 mm.

Since the force sensor is placed between the micrometer travel translator and the cylindrical joint, the deformation of the force sensor perturbs the measurement of the beam end-shortening which should be fixed. In order to avoid this drawback, we impose the maximum deflection at the beam center in its post-buckling regime with zero actuating force. The beam camber is then fixed at 13 mm which corresponds to an end-shortening of 0.22 mm accounting for the compression of the force sensor. When an actuating force is applied to the buckled beam, the vertical displacement of its point of application is monitored very carefully step by step. At each displacement of the actuating force in the direction perpendicular to the beam axis, we measure the voltage at the output of the amplifier of the SM2 force sensor and convert it to Newtons.

Regarding the measurement of the actuating force, we control the displacement of the point of application by placing the beam between two parallel cylinders which have been machined to form a sharp edge on the half part of the cylinders. Fig. 4 shows the detailed section of the actuating device with the cylinders. Using such a device, we are able to control the displacement and to apply the actuating force in both directions (from top to bottom and *vice versa*). Moreover, the friction and damping effects during the switching process are minimized. The device is controlled by two-axis translators with the perpendicularity between the two axes of translation motion. This allows us to control the position of the actuating force along the beam axis and the other translator stage guides the position of the point of applied force along the direction perpendicular to the beam axis. The control is achieved with a perfect accuracy around 1 μm. The applied actuating force is measured by using a force sensor with the LSB200 model from Futek® (an S-shaped force sensor with four strain gauges). Alike the force sensor for the measurement of the axial force, the sensor is connected also to an amplifier for the conversion of the force sensor output into voltage. Contrary to the force sensor measuring the compressive force, in this case we do not need to account for the deformation of the sensor, since the sensor deformation is not perceptible for the range of concerned forces.

3.2. Experimental results

3.2.1. Diagram of bifurcation

Among the first results are the tests for the bifurcation diagram for the elastic buckled beam. The measurement procedure is rather easy. We use the travel translator to impose an end-shortening at the right end of the beam and we read directly on the micrometer the translation. The second measurement is the beam deflection at its center. At this end, a micrometric translator is used vertically. The continuity function of a multimeter allows us to detect the contact between the beam center deflection and a small wire fixed at the vertical translator. For each amount of axial translation the maximum deflection is read on the micrometer of the vertical translator. Fig. 5 shows the bifurcation diagram, that is the deflection at the beam center as a function of the end-shortening. We have two curves; the continuous line corresponds to the numerical results coming from the model which has been presented in Camescasse et al. (2013). The red spots are for the measurement. We observe good results between the model and experimental data. Obviously, because of the high slenderness ratio of the beam $\frac{L}{h} = 500$, the pre-buckling zone (for compressive force less than the critical buckling force) is not observable.

3.2.2. Bistable response for mid-span actuation

The aim of the Section is to experimentally characterize the actuating force as a function of the beam deflection according to the location of the applied force. Two cases are examined: (i) actuation at the beam mid-span and (ii) off-center actuation.

The experimental set-up allows us to obtain two quantities as a function of the vertical position of the applied force: (i) the compressive force P for a given end-shortening and (ii) the actuating force F. Both forces P and F are considered as shooting parameters for the differential equation governing the cross-section rotation Eq. (2). We recall that since the end-shortening is given, the compressive force P is accordingly unknown and it is changed with the actuating force F. The experimental results are presented in Fig. 6. The curves show the variation of the compressive force while the beam is switching from one stable position to the other.
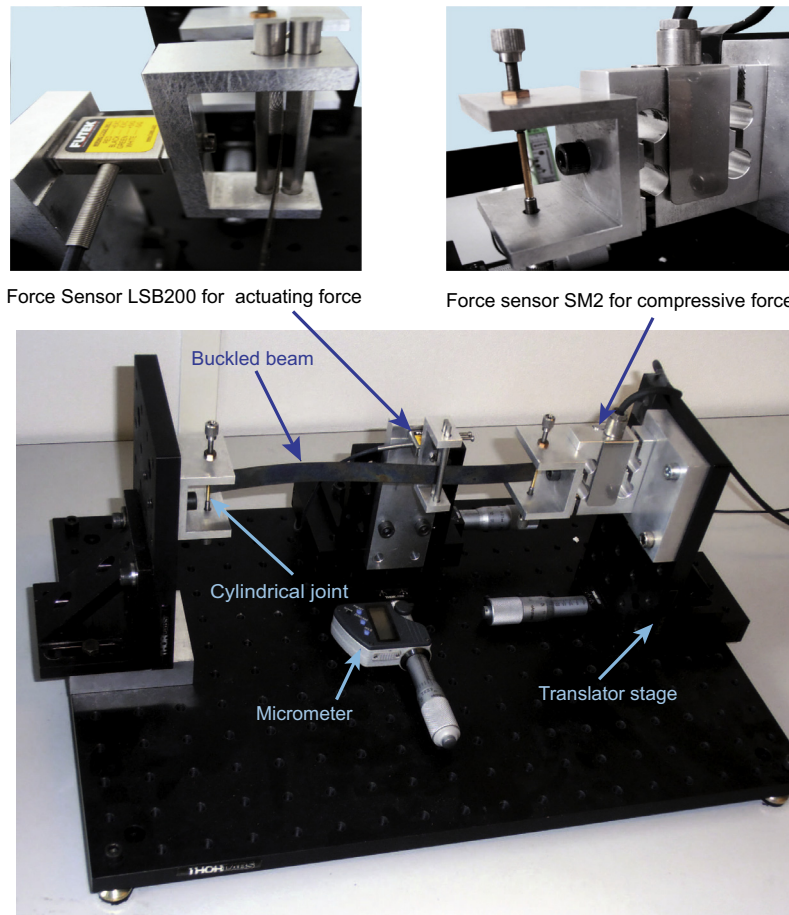
Force Sensor LSB200 for actuating force

Force sensor SM2 for compressive force

Buckled beam

Cylindrical joint

Micrometer

Translator stage

Fig. 2. Experimental set-up exhibiting the force sensors for the measurement of the buckling and actuating forces while the buckled beam is switched.
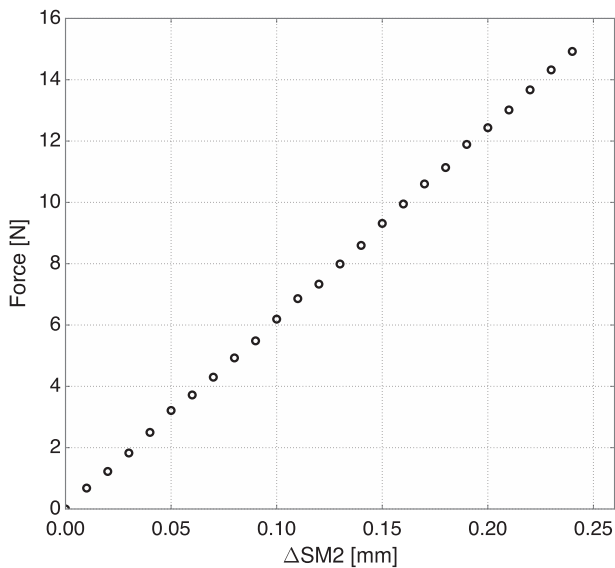

Fig. 3. Compensation curve of the force sensor SM2 for the compressive force measurement: force as a function of sensor deformation.

Caliper

Cylinders

Beam

Fig. 4. Actuating device: details showing the beam placed between two cylinders with sharp edges.

In Fig. 6 two series of experimental data are shown: (i) the red circles correspond to the switching from the top stable position to the lower one and (ii) the blue circles are for the switching in the reverse direction (from bottom to top). The continuous black line depicts the results from the numerical simulation of the bistable
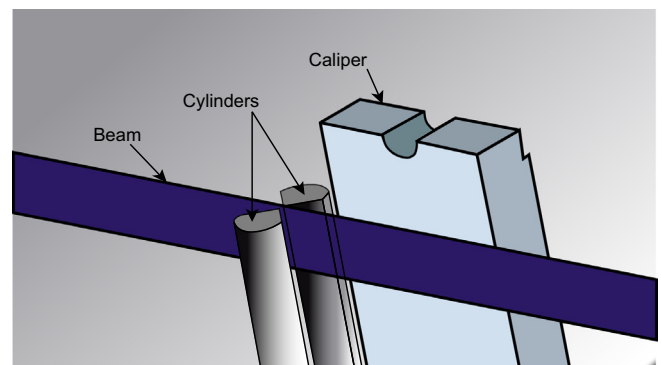
equations Eq. (2). First of all, we observe that the experimental points are very close to the analytical results, leading to a good validation of the proposed model. Nevertheless, we notice very clearly in the experimental results a jump in the switching direction corresponding to a small increase in the compressive force. The jump appears at the beginning of the switching phase and around the bifurcation point (b) in Fig. 6a. More precisely, this jump is due to the rapid appearance of the third buckling mode. As matter of fact, the switching from the buckling mode 1 to that of mode 2 via the mode 3 produces a small increase in the compressive force which is rapidly released. We observe a rapid transition (jump) from the third buckling mode to the second one. In spite of the
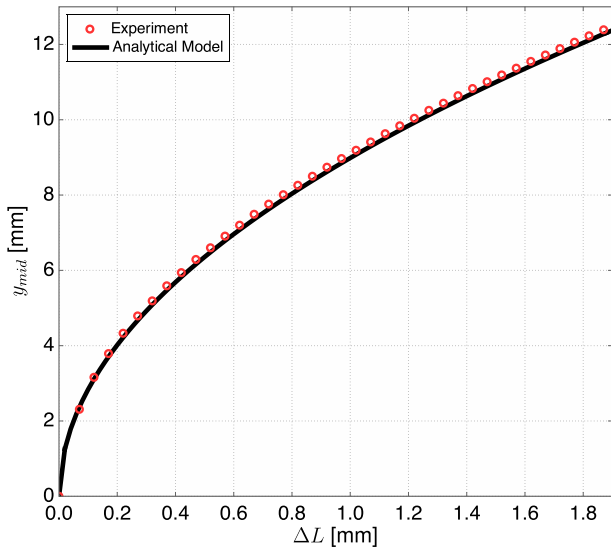
Fig. 5. Beam deflection at its center as a function of the end-shortening: result from model (continuous black line) and experimental data (red circles). (For interpretation of the references to color in this figure legend, the reader is referred to the web version of this article.)

jump phenomenon which has not been predicted by the model, the comparison between the analytical results and experimental data remains good (less than 7 % including disparities due to jumps).

A second result extracted from experimental study is the bistable response: an actuating force as a function of the beam center displacement. For the experimental tests we use the LSB200 force sensor from Futek®. The force is measured while the point of actuation on the beam moves along a direction perpendicular to the beam axis at the beam mid-span. The results are shown in Fig. 6b where the analytical/numerical results (in continuous line) and data from the measurement (blue and red circles) are superimposed. Similar to the compressive force as a function of the mid-span beam displacement, a jump is observed around the bifurcation point (*b*) from mode 1 to mode 2 when going from the bottom to the top. This sudden jump is due to the appearance of the third buckling mode and a jump from mode 3 to mode 2 is

observed. The jump is also observed for the switching from upper to lower stable positions. The colors of the circles and the letters referred to the same events as in Fig. 6a. The results of the experimental tests are coherent, which validates the proposed modeling. The error between the analytical and experimental results is around less than 9 %.

In Fig. 7, a series of photos are presented to capture the switching scenario. Foremost, we want to determine the role of the buckling modes played on the switching process. Each photo is assigned by a letter on the response diagrams: (i) compressive force versus displacement (Fig. 6a) and (ii) actuating force versus the beam mid-span displacement (Fig. 6b). We start with buckling mode 1 (photo (a) in Fig. 7). The chronology continues with photo (b) where we can observe the combination of modes 1 and 3. Photo (c) shows the beam deformation just after the jump from mode 3 to mode 2. Photo (d) shows clearly a pure buckling mode 2 and finally the second stable configuration of the bistable beam is reached as shown in photo (f) passing before through the intermediate state depicted by photo (e).

3.2.3. Off-center actuation

In this part, we want to examine the influence of the force offset on the force measurement at the bifurcation point of bistable response branches. The critical force depends on the ratio δ. The end-shortening is fixed at 1 % of the beam length at rest, that is 2 mm. The measurement procedure is identical to the mid-span actuation. Nevertheless, the measurement of the actuating force is not complete. Once the bifurcation force is detected, the process is stopped and the actuating force is set to zero. More precisely, using the bistable response of the analytical study (actuating force as a function of its vertical position), the force at the bifurcation point is obtained when the path in the force–displacement response changes from a stable branch to an unstable one and *vice versa*. The measure of the force closest to the bifurcation point is then retained for the diagram. The process continues with an another value of δ. Fig. 8 exhibits the final results. Red circles are the measurement while the continuous black line derives from the analytical model. The result is symmetric with respect to the vertical $\delta = 0.5$. The experimental results presented in Fig. 8 look like a cloud of points spread out around the theoretical curve. Nevertheless, the main discrepancy with respect to the numerical simulation is less than 5%. Moreover, the minimum bifurcation
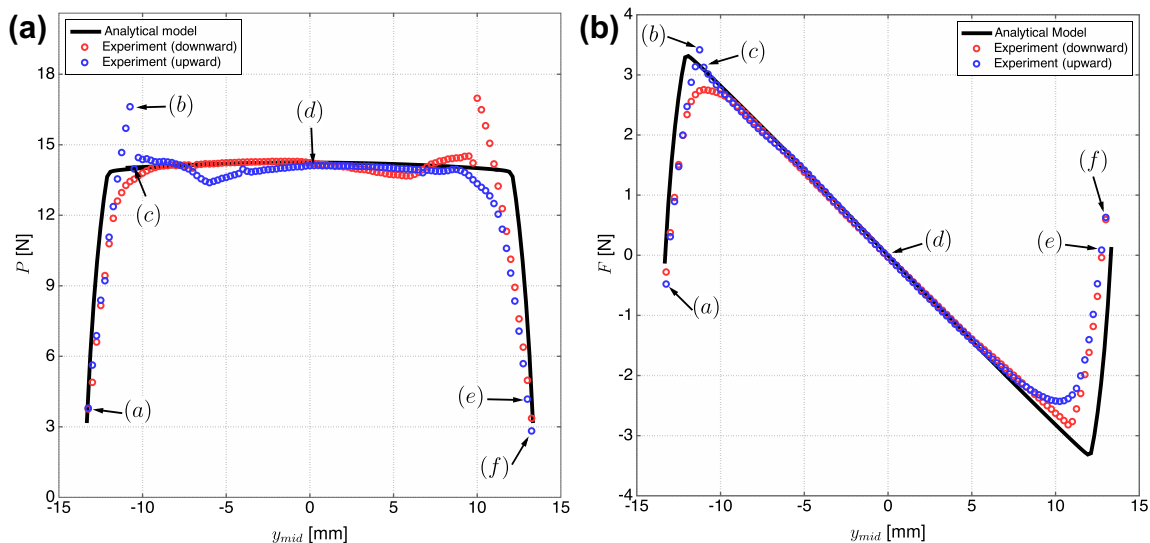

Fig. 6. Mid-span actuation: experimental results and comparison to the model (a): compressive force vs displacement of beam center, (b): actuating force as a function of mid-span displacement.
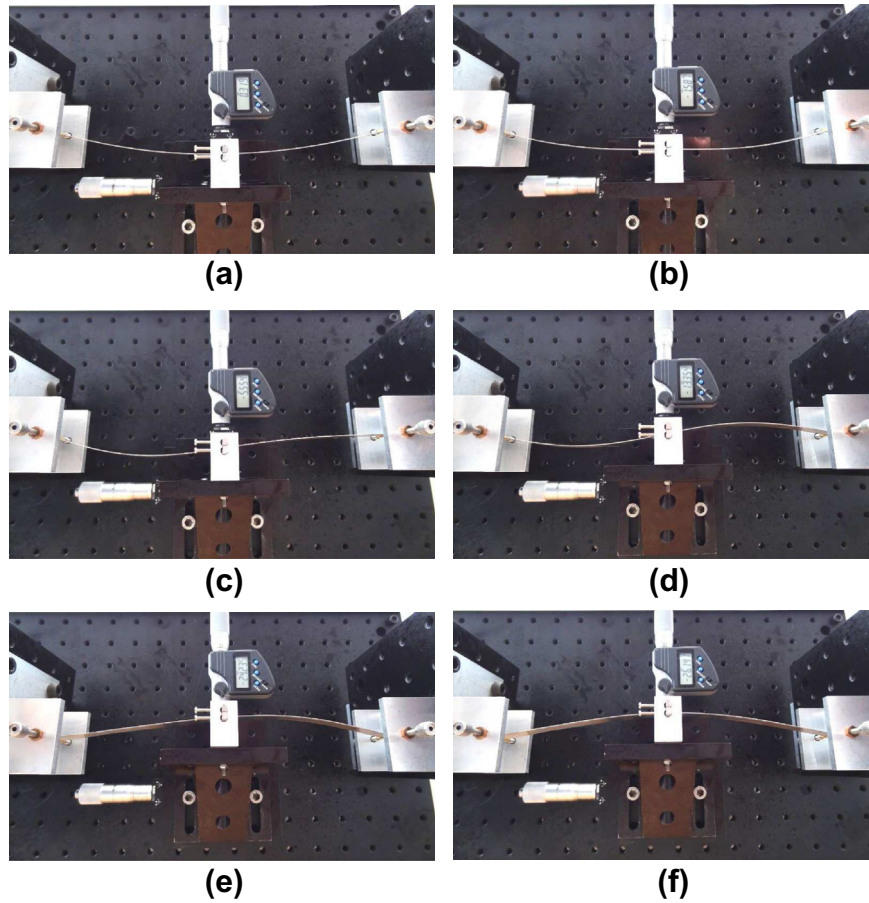
Fig. 7. Chronology of a centered actuation (the letters are referred to those of the curves in Fig. 6a and b).
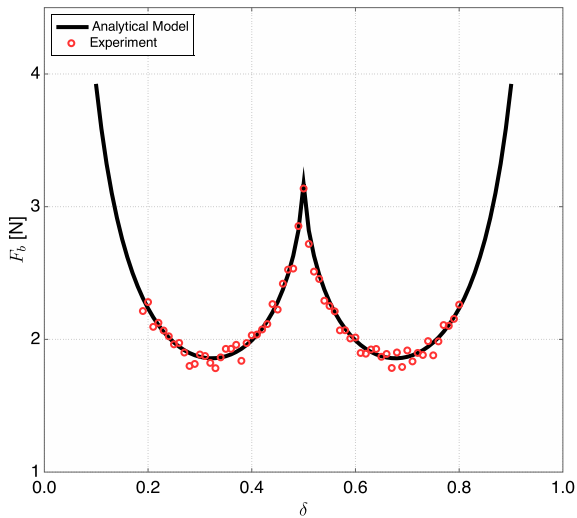

Fig. 8. Force at the bifurcation point as a function of the force off-set.

force is located at about $\delta = 0.3$ for a slenderness $\frac{L}{h} = 500$. In spite of the relative difficulty of the measurement, a very good agreement with the results is obtained.

The variation of the compressive force and actuating force as a function of the vertical displacement y_C of the point C are examined in the same way as the mid-span actuation situation. The procedure is strictly identical, yet, we take $\delta = 0.4$ for the force off-set. The experimental data and the results of the numerical

simulations are plotted together in Fig. 9. The first result concerns the compressive force P as a function of the vertical displacement y_C. The curves are drawn in Fig. 9a. It is mainly observed that the situation is somewhat different from that of the mid-span actuation. As a matter of fact, the non-symmetrical loading does not trigger the buckling mode; only the modes 1 and 2 are considered. Moreover, mode 3 which is symmetrical cannot be obtained with such a loading. According to the modeling part of the present work (Camescasse et al., 2013), for an off-center actuation the beam begins to switch using the second buckling mode. The effect is clearly exhibited in Fig. 9b for the bistable response: actuating force versus displacement. In both Fig. 9a and b the red circles correspond to the switching from upper to lower positions and those in blue for the switching back. Moreover, the chronology of the beam switching is given by the series of photos in Fig. 10. The letters are reported in Fig. 9a and b. The process starts with the stable position - the buckled beam at the upper position (see photo (a) in Fig. 10). As the vertical position y_C of the actuating force is lowered towards the second stable position, we observe the deformation of the beam consisting in a combination of buckling modes 1 and 2. Photos (b), (c) and (d) clearly exhibit that mode 2 becomes predominant until the beam almost fits with a pure buckling mode 2 (see photo (d)). The sequence of the process continues now for $y_C < 0$ (see photos (e) and (f)). At the point (f) in Fig. 9a and b, the beam undergoes a small jump from the branch of mode 2 to that of mode 1. The actuating force decreases towards zero and the buckled beam reaches its lower stable position (photo (f)). Contrary to the mid-span actuation, the paths in back and forth directions are different as shown in Fig. 9a and b (curves with red and blue circles).
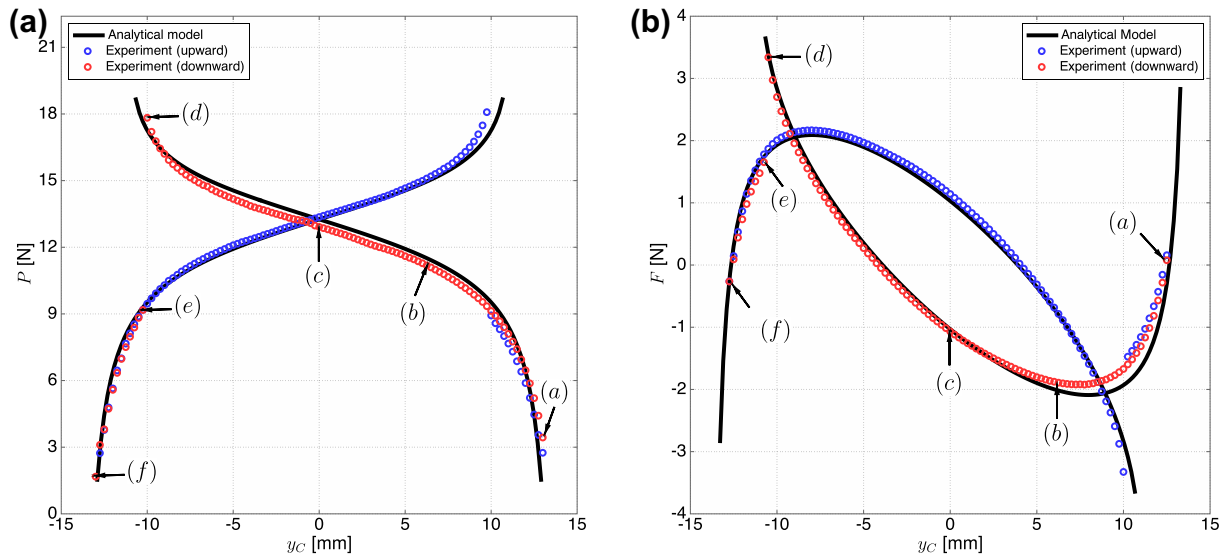
Fig. 9. Off-center actuation: experimental results and comparison to the model (a): compressive force vs the displacement, (b): actuating force as a function of the force displacement.
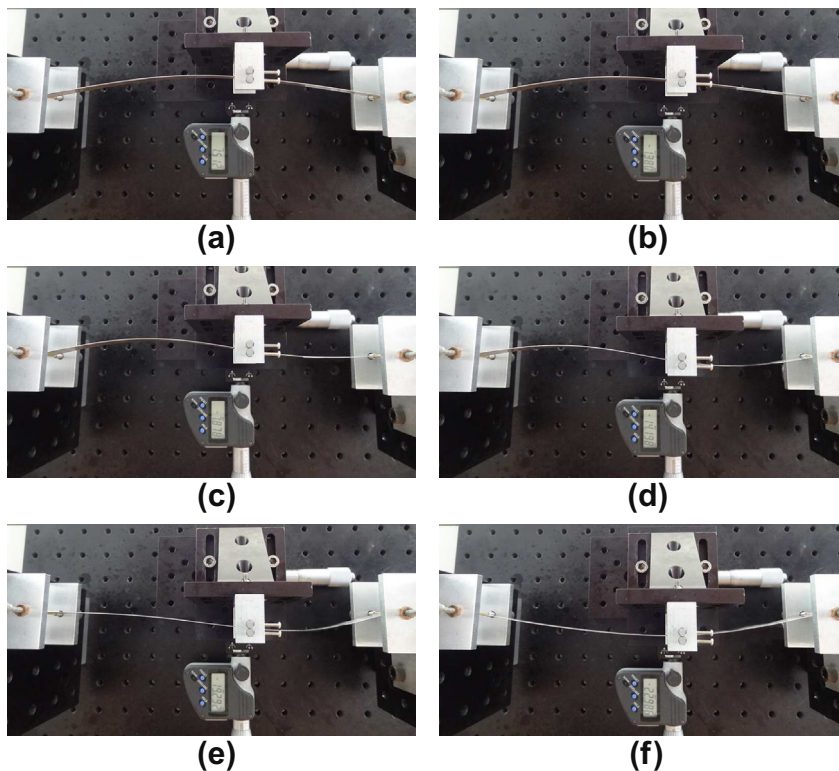

Fig. 10. Chronology of an off-center actuation (the letters are referred to those of the curves in Fig. 9a and b).

4. Discussion and concluding remarks

The main results of the experimental tests presented in the previous section have proved the validity of the proposed modeling based on the elastica approach. The experimental study allows us to clarify the role played by buckling modes on the switching scenario. The comparison between the experimental measurements and the numerical results is good and the discrepancies remain small.

It is worthwhile underlining that the pre-buckling regime for which the compressive force is less than the critical force (buckling force) is not shown on the bifurcation diagram (see Fig. 5). The reason for that is that the buckling phenomenon starts for an infinitesimal amount of end-shortening (few micro-meters). Moreover, the beam is not perfect and the slightest defect causes the buckling to start. In the analytical part of the work the numerical simulations have been performed for different slenderness ratios so that the pre-buckling regime is clearly identified.

The experimental results reported in the present work can be easily compared to those obtained by Cazottes et al. (Cazottes et al., 2010) for similar situation, but with a clamped–clamped buckled beam. In Cazottes' work, the model used is quite different

from ours; it is based on the truncated buckled mode expansion and the beam extensibility is accounted for. In fact, it is the extensibility which produces the nonlinearity of the model; the latter is a weak version of the "elastica" model. Even if the tested beams and the boundary conditions are different, it is interesting to note that the numerical and experimental results, in their essence, are very similar to a scaling factor. By way of conclusion, a good correspond is observed between the bistable beam response modeling prediction and the experimental results, which establishes a reliable validation of the model.

A complementary and forthcoming work would be to study the vibration of the bistable beam in the post-buckling regime (vibration of small amplitude around the buckled state). The experimental validation of the vibrating behavior of the buckled beam will be considered as well.

References

Baker, M.S., Howell, L.L., 2002. On-chip actuation of an in-phase compliant bistable micro-mechanism. J. Microelectromech. Syst. 11, 566–573.

Camescasse, B., Fernandes, A., Pouget, J., 2013. Bistable buckled beam: elastica modeling and analysis of static actuation. Int. J. Solids Struct. 50 (19), 2881–2893.

Cazottes, P., Fernandes, A., Hafez, M., Pouget, J., 2010. Bistable buckled beam: modeling of actuating force and experimental validations. ASME J. Mech. Des. 131, 1001001–1001011.

Charlot, B., Sun, W., Yamashita, K., Fujita, H., Toshiyoshi, H., 2008. Bistable nanowire for micromechanical memory. J. Micromech. Microeng. 18, 045005 (7 pp.).

Chen, J.-S., Hung, S.-Y., 2011. Snapping of an elastica under various loading mechanisms. Eur. J. Mech. A. Solids 30, 525–531.

Chen, J.-S., Su, Y.-H., 2011. On the use of an elastic-slider assembly as a bistable device. Mech. Mach. Theory.

Das, K., Batra, R.C., 2009. Pull-in and snap-through instabilities in transient deformations of microelectromechanical systems. J. Micromech. Microeng. 19, 035008 (19 pp.).

Edwards, B.T., Jensen, B.D., Howell, L.L., 2001. A pseudo-rigid body model for initially-curved pinned-pinned segments used in compliant mechanisms. ASME J. Mech. Des. 123 (3), 464–468.

Goll, C., Baker, W., Buestgens, B., Maas, D., Menz, W., Schomburg, W.K., 1996. Microvalves with bistable buckled polymer diaphragms. J. Micromech. Microeng. 6 (1), 77–79.

Gray Jr., G.D., Kohl, P.A., 2005. Magnetically bistable actuator part 1. ultra-low switching energy and modeling. Sens. Actuators A 119, 489–501.

Gray Jr., G.D., Prophet, E.M., Zhua, L., Kohla, P.A., 2005. Magnetically bistable actuator part 2. fabrication and performance. Sens. Actuators A 119, 502–511.

Howell, L.L., Midha, A., Norton, T.W., 1996. Evaluation of equivalent spring stiffness for use in a pseudo-rigid-body model of large-deflection compliant mechanisms. ASME J. Mech. Des. 118 (1), 126–131.

Jensen, B.D., Howell, L.L., 2004. Bistable configurations of compliant mechanisms modeled using four links and translational joints. ASME J. Mech. Des. 126, 657–666.

Jensen, B.D., Howell, L.L., Salmon, L.G., 1999. Design of two-link in-plan, bistable compliant micro-mechanisms. ASME Mech. Des. 12 (3), 416–423.

Maekoba, H., Helin, P., Reyne, G., Bourouina, T., Fujita, H., 2001. Self-aligned vectical mirror and V-grooves applied to an optical-switch: modelling and optimization of bistable operation by electromagnetic actuators. Sens. Actuators A 87 (3), 172–178.

Matoba, H., Ishibawa, T., Kim, C., Muller, R.S., 1994. A bistable snapping mechanism. IEEE Micro-Electro-Mech. Syst. 45–50.

Park, S., Hah, D., 2008. Pre-shaped buckled-beam actuators: theory and experiments. Sens. Actuators A 148, 186–192.

Pippard, A.B., 1990. The elastic arch and its modes of instability. Eur. J. Phys. 11, 359–365.

Qiu, J., Lang, J.H., Slocum, A.H., 2001. A centrally-clamped parallel-beam bistable MEMS mechanism. In: Proceeding of 14th IEEE International Conference on Micro Electro Mechanical Systems, pp. 353–356.

Saif, M.T.A., 2000. On a tunable bistable MEMS – theory and experiment. J. MEMS 9 (2), 157–169.

Schomburg, W.K., Goll, C., 1998. Design optimization of bistable micro-diaphragm valves. Sens. Actuators A 64 (3), 259–264.

Vangbo, M., Bäklund, Y., 1998. A lateral symmetrically bistable buckled beam. J. Micromech. Microeng. 8, 29–32.